COPPER MINERALIZATION IN PENNSYLVANIAN-PERMIAN ROCKS OF THE TONTO RIM SEGMENT OF THE MOGOLLON RIM IN CENTRAL ARIZONA

by

Ralph David Rogers

A Thesis Submitted to the Faculty of the

DEPARTMENT OF GEOSCIENCES

In Partial Fulfillment of the Requirements
For the Degree of

MASTER OF SCIENCE

In the Graduate College

THE UNIVERSITY OF ARIZONA

1 9 7 7

STATEMENT BY AUTHOR

This thesis has been submitted in partial fulfillment of requirements for an advanced degree at The University of Arizona and is deposited in the University Library to be made available to borrowers under rules of the Library.

Brief quotations from this thesis are allowable without special permission, provided that accurate acknowledgment of source is made. Requests for permission for extended quotation from or reproduction of this manuscript in whole or in part may be granted by the head of the major department or the Dean of the Graduate College when in his judgment the proposed use of the material is in the interests of scholarship. In all other instances, however, permission must be obtained from the author.

SIGNED: Ralph R Ryan

APPROVAL BY THESIS DIRECTOR

This thesis has been approved on the date shown below:

Spencer R Titley

S. R. TITLEY
Professor of Geology

12 Dec 77

Date

ACKNOWLEDGMENTS

The completion of this work would have been impossible without the assistance of many people. I wish particularly to thank the members of my committee: Drs. Titley, Peirce and Norton for their invaluable guidance through all phases of this study. Dr. Schumacker offered valuable assistance in the early portions of this study. Mr. Nile Jones was an invaluable co-worker while doing field work during the summer of 1975.

Financial assistance was provided for this study by the U. S. Geological Survey under Grant No. 14-08-0001-G-147, given to the Arizona Bureau of Mines, The University of Arizona, H. Wesley Peirce principal investigator. Funds of computer time were provided by the Department of Geosciences, The University of Arizona.

TABLE OF CONTENTS

TABLE OF CONTENTS--CONTINUED

LIST OF ILLUSTRATIONS

ABSTRACT

Stratabound sulfide mineralization and associated organic material in the lower portion of the Supai Formation along the Mogollon Rim occurs in micrites, quartz arenites and limestone pebble conglomerates. Pyrite, bornite, chalcopyrite, chalcocite and covellite, occur as individual minerals and as mineral aggregates. Textural relationships suggest that chalcocite and bornite replaced pyrite, bornite was replaced by chalcopyrite and chalcocite, bornite and chalcopyrite replaced chalcocite in addition to co-precipitation of bornite and pyrite or chalcocite $\pm$ chalcopyrite.

Local groundwater or brines have been considered as possible solutions from which the sulfides were deposited. Thermochemical data for aqueous species at 25°C and 1 atm and irreversible mass transfer calculations of reactions between the solutions and rocks containing 60 percent calcite, 35 percent quartz and 5 percent pyrite predict that 6.36×10^{-5} grams of Cu/Kg of H_2O could have been introduced into the rock by brines and 1.16×10^{-8} grams of Cu/Kg of H_2O by groundwater. Mineralization at one locality could have been produced by 1.18×10^{8} liters of brine or by 6.20×10^{11} liters of groundwater. Preliminary calculations suggest that the mineralization could have been completed by the brine in 4.44×10^{5} years while the groundwater would take over 3 billion years, suggesting that transportation and deposition by the brine is more likely.

INTRODUCTION

Paleozoic rocks are exposed along the Mogollon Rim which forms a northwest trending topographic escarpment in central Arizona. It is the southern edge of the Colorado Plateau physiographic province. A copper occurrence in the Rim area was first reported by Ransome (1916).

Subsequent investigation has shown copper sulfides and oxides to occur in three principal localities: 1) Fossil Creek Canyon, 2) Promontory Butte, and 3) Turkey Mountain (Fig. 1). Minor lead, zinc, silver, and uranium are associated with the copper. Mineralization occurs in conglomerates and related rocks. These rocks have been assigned to the lower portion of the Supai Formation by Ross (1973).

The purpose of this study was to investigate the geology of the mineralization so as to better understand the processes and timing involved in the emplacement of the sulfide minerals. The area of study is in Gila County and focuses on the Tonto Rim portion of the Mogollon Rim (Fig. 1). Outcrop is limited by an extensive cover of pine and/or chapparal.

Stratigraphic sections were measured, described, and sampled at the three mineralized localities. Lateral extent and continuity of rock units and mineralization were determined. Petrographic studies were made of polished surfaces and thin sections of mineralized specimens. Groundwater and/or brines from an ancestral Holbrook Basin have been considered as possible solutions from which the sulfides were deposited. Thermochemical data for aqueous species at 25°C and 1

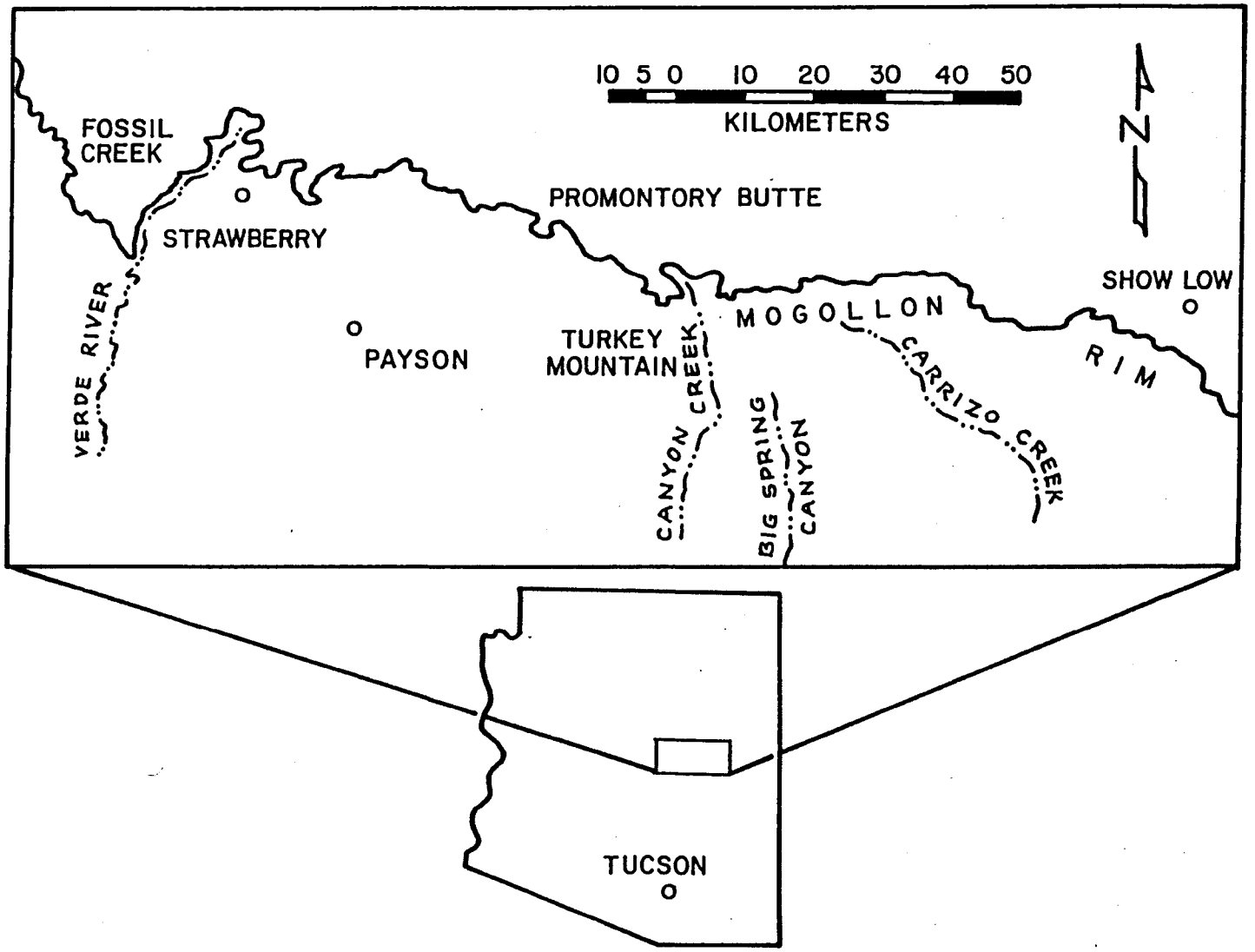

Fig. 1. Location Map

Showing Tonto Rim portion of the Mogollon Rim.

atmosphere, and irreversible mass transfer calculations of reactions between these solutions and the host rocks were studied.

Previous Investigations

Ransome (1916) briefly discussed the Paleozoic section exposed in Fossil Creek. Huddle and Dobrovolny (1945) conducted a regional study which unified stratigraphy along the Mogollon Rim and projected it beneath the Mogollon slope and into the Holbrook Basin subsurface. Jackson (1951) studied the stratigraphy and environment of deposition of the Supai Formation along the Rim. McGoon (1962) reported on the cupriferous carbonaceous beds at Fossil Creek and noted a similar occurrence at Promontory Butte. Brew (1965) studied the stratigraphy and environment of deposition of the Naco Formation in central Arizona. Ross (1973) studied the Pennsylvanian and Early Permian depositional history in central and southeastern Arizona. Conyers (1975) studied the depositional environments of the Supai Formation in central Arizona. Peirce, Jones, and Rogers (1977) studied the mineralization and stratigraphy of Paleozoic rocks in the Mogollon Rim and Slope region. The present study is an outgrowth of that work.

REGIONAL GEOLOGY

Precambrian rocks are exposed immediately to the south of the Mogollon Rim. Older Precambrian rocks include green schist and granites which have not been mapped in detail. Also of Older Precambrian age are rocks of the Mazatzal Quartzite. Of interest to this study are two exposures of this formation, termed Pine and Christopher Islands by Teichert (1965). It is likely that the resistant quartzites of these islands were topographically positive features at least through Mississippian time as Pennsylvanian Naco Formation is found to overlie them in sedimentary contact. The extent to which these features have affected local stratigraphy is not entirely clear, but they could have influenced later events.

The Younger Precambrian is represented by the Apache Group, Troy Quartzite, and diabase. The Apache Group is made up of three formations which are, from bottom to top, Pioneer Shale, Dripping Spring Quartzite, and Mescal Limestone. The lithology and distribution of these units are discussed in detail by Shride (1967). The Pioneer Shale is predominantly a tuffaceous siltstone or silty mudstone and ranges from 50 to 175 meters in thickness. The Dripping Spring is predominately made up of arkose, feldspathic quartzite, and feldspathic siltstone ranging from 150 to 250 meters in thickness. The Mescal Limestone is made up of limestones, dolomites, and argillites, some of which have been silicified and/or metamorphosed to calc-silicate minerals. The thickness of the Mescal Limestone varies from 80 to 150

meters. The Apache Group is intruded by diabase sills that have been dated at 1140 ± 40 m.y. by K-Ar and at 1200 m.y. by zircons (Shride 1967). The Troy Quartzite is made up of arkose, pebbly quartz sandstone, and medium to coarse grained quartzite. It attains a maximum thickness of 400 meters. These Younger Precambrian rocks are exposed in the Sierra Ancha Mountains 40 to 50 kilometers south of the Rim. They wedge out along a positive edge that trends approximately N30E and intersects the Rim near Promontory Butte.

Paleozoic rocks exposed along the Rim include Cambrian, Devonian, Mississippian, Pennsylvanian, and Permian sedimentary rocks. Interesting variations are seen in the lithologies of these rocks, both in the east-west sense along the Rim and in the north-south sense normal to the trend of the Rim.

The base of the Paleozoic section is made up of medium-to-coarse grained sandstones which are locally conglomeratic or arkosic. These rocks are generally unfossiliferous and considerable disagreement has arisen as to their age. Some workers have assigned at least some of these rocks to the Tapeats sandstone of Cambrian age, e.g., Huddle and Dobrovolny (1952). Others have assigned all of these rocks to the Devonian Martin Formation, e.g., Teichert (1965). Recent paleomagnetic investigations by Elston and Bressler suggest that the two lowest units in Teichert's East Verde River section, units 1 and 2 of the Beckers Butte Member (p. 145), are in fact Cambrian in age (Bressler 1977, personal communication). No rocks of Silurian and Ordovician age are recognized in this region.

The Devonian Martin Formation is made up of dolomites and some limestone and varying amounts of sandstone, siltstone, and shale. Thickness trends are varied. Along the Rim, thicknesses vary from 0 to 100 meters, with Christopher and Pine Islands showing a direct influence on sedimentation resulting in local non-deposition. To the northeast, in the subsurface, Devonian rocks wedge out onto the Defiance positive (Teichert 1965). To the south and west, thicknesses of 170 meters are obtained.

The Mississippian Redwall Limestone is a light gray to white limestone. Characteristically, the top of the unit is a solution breccia with blocks of limestone surrounded by red siltstone and chert. The solution breccia is the result of post-Redwall, pre-Naco erosion. The Redwall thins to a few meters in thickness in the area of Canyon Creek and thickens to over 30 meters to the east and west along the Rim. The Redwall is absent over the Precambrian Quartzite islands. From the Rim to the north and south, Mississippian limestones thicken to over one hundred meters. To the northeast, the Redwall wedges out on the Defiance positive (McKee and Gutschick 1969).

Pennsylvanian rocks that outcrop along the Mogollon Rim have been assigned to the Naco Formation by Brew (1965) and the Horquilla Formation by Ross (1973). Brew divided the Naco into three informal members: Alpha, Beta, and Gamma. The Alpha consists of basal unstratified beds of the regolith produced during the formation of the karst topography on the underlying Redwall. The overlying stratified rocks of the Alpha Member are clastic siltstones and mudstones which grade

into the Beta Member vertically. The Beta Member is made up of alternating limestones and shales, many of which contain marine fossils. To the northwest along the Rim, this member is characterized by more reddish clastic intervals, which have been interpreted as a shoreward facies (Brew 1965).

The Gamma Member overlies the Beta with a gradational contact. It is made up of a gradational sequence showing intertonguing of marine limestones or shales lying to the southeast with non-marine sandstones and siltstones lying to the northwest (Brew 1965).

The contact between the Naco Formation and the Supai Formation is perhaps best considered as gradational. It is characterized by intercalated red sandstones and gray limestones. This has led various workers to assign the contact at either the first of the red beds or the last of the limestones in the sequence. This leads to problems when discussing the thickness and correlation of the units involved. For this study, the measurements and definitions of Brew (1965) have been used.

Thickness of the Naco varies markedly. In Fossil Creek, the formation is approximately 140 meters thick (Brew, 1965). The next location to the east where a complete section has been measured is Big Spring Canyon on the Fort Apache Indian Reservation. At this location, the Naco is over 300 meters thick and this thickening trend continues to the southeast (Brew 1965).

North of the Rim, subsurface data show that the limestones and shales of the surface exposure grade into redbed clastics. Lokke

(1962) studied fusulinids from both surface and subsurface rocks and concluded that the Naco thinned significantly to the north from the Rim, due to nondeposition.

To the northeast, the Naco depositionally wedges out against the Defiance positive and in several wells Supai is found unconformably overlying Precambrian basement. In Carrizo Creek, conglomerates of the Gamma member are arkosic and contain coarse quartz grains. The most probable explanation is that the feldspar and coarse quartz were derived from Precambrian rocks, then exposed on the Defiance positive. West of Cibeque, correlative conglomerates contain only trace amounts of feldspar and fine-grained quartz.

The Naco of the Rim area has been interpreted to represent the transgression of Pennsylvanian seas from the southeast during mid-Pennsylvanian time with subsequent regression during Later Pennsylvanian time (Brew 1965). This paleobasin has been referred to by Brew (1965), and others, as the Pedraqosa Basin.

The placement of the Pennsylvanian-Permian boundary is difficult due to the paucity of fossil data. Desmoinesian fusulinids have been found in the lower portion of the Naco formation in Fossil Creek by Huddle and Dobrovolny (1945). Plant fossils are present in the Oak Creek Member of Jackson (1951) at Promontory Butte. These were studied by Blazey (1971) who concludes that they are probably of Wolfcampian age although absolute data are lacking. Ross has found Wolfcampian fusulinids in rocks which he would correlate with Jackson's Oak Creek

Member. The evidence suggests that the Pennsylvanian-Permian boundary is somewhere near the base of the Oak Creek Member.

Rocks of Permian age include the Supai Formation and the Coconino Sandstone. They are characterized predominately by clastic sedimentary rocks. The lower portion of the Supai Formation is characterized by sandstones, siltstones, and thin but seemingly important conglomerates. In the region of study, these rocks exhibit cut and fill features, point bars, and overbank deposits characteristic of fluvial environments of deposition. The upper part of the Supai is characterized by sandstones and siltstones with several interbedded dolomitic limestones. The largest of these is the Fort Apache Limestone which has been given member rank by Winters (1963) and is a marker unit all along the Mogollon Rim from Oak Creek Canyon to the Fort Apache Indian Reservation. The Supai is approximately 500 meters thick.

The Supai Formation is conformably overlain by the Coconino Sandstone of Permian age. In the Tonto Rim region, the Coconino is an eolian sandstone, approximately 200 meters thick. The Coconino is conformably overlain by the Kaibab Limestone. Lithologically, the Kaibab is a sandy limestone and ranges in thickness from 0 to 150 meters (McKee 1938).

To the south, Permian rocks have been removed by post-Paleozoic erosion throughout most of east-central Arizona. To the north, the Supai thickens to over 600 meters and contains evaporite deposits, predominately, in the upper portion above the Fort Apache Limestone.

These consist of thick accumulations of gypsum, anhydrite, halite, and some potash.

Rocks of Mesozoic age are limited to local occurrences of Triassic and Cretaceous sedimentary rocks. Scattered remnants of Triassic clastic rocks of the Moenkopi and Chinle formations are preserved in the Tonto Rim region. To the east, the Triassic rocks are overlain by marine sedimentary rocks of Cretaceous age. The Cretaceous rocks are the Dakota Formation, Mancos Shale, and Mesa Verde Formation. Prior to deposition of the Cretaceous rocks, the entire region was tilted to the northeast as evidenced by the fact that the Cretaceous rocks sit on progressively older rocks from north to south. Intrusive activity associated with major copper mineralization took place during Laramide time 100 km south of the Rim, near Globe and elsewhere in Arizona.

Rocks of Cenozoic age include conglomerates of continental origin and volcanic rocks. Several conglomerates of Lower to Middle Tertiary and younger age are found along the Rim. Volcanism in the area is restricted to the Late Tertiary. A K-Ar date of 14 m.y. on a Tuff breccia at the base of the Hackberry Mountain sequence, west of Fossil Creek, was obtained by Sabels (1962). Basaltic flows from 12 to 6 m.y. (personal communication, M. Shafiqullah 1977) old are common in the area of Fossil Creek.

The Diamond Rim Fault is the major structural feature which controls the location of the Mogollon Rim in the study area. The Diamond Rim Fault is a normal fault with a displacement of 300 to 500

meters (Titley 1962). The fault cuts Tertiary conglomerates and is overlain by unfaulted basaltic flows. The fault is probably of Basin and Range age.

STRATIGRAPHY

The lower portions of the Tonto Rim region are characterized by large amounts of cover and relatively poor outcrops of the more incompetent rocks. Mineralization occurs in this incompetent zone and, therefore, exposures tend to be limited. The absolute tracing of strata for long distances is not possible. This leads to the conclusion that the stratigraphic location of mineralized rocks must be studied in general terms.

The Fort Apache Limestone and the Redwall Limestone are marker units that are exposed along the Rim. These units are used here to locate, stratigraphically, the rocks containing mineralization. Limestone pebble conglomerates are the most distinctive lithology associated with the mineralized occurrences. Limestone pebble conglomerates in the Paleozoic section are restricted to the lower Supai-upper Naco interval. Stratigraphic measurements were made at the three mineralized localities (Fossil Creek, Promontory Butte, and Turkey Mountain) and at Big Spring Canyon. The Big Spring Canyon section is included because the entire section from Redwall to the Fort Apache is well exposed. These measurements are shown on Fig. 2. Because of the large amount of cover at Turkey Mountain and Promontory Butte, there is the possibility that faulting could have disrupted the section. The section from the conglomerates to the Fort Apache was not measured at Turkey Mountain because faulting in this section is likely. It should be noted that the thickness of the conglomerate-bearing sequence is

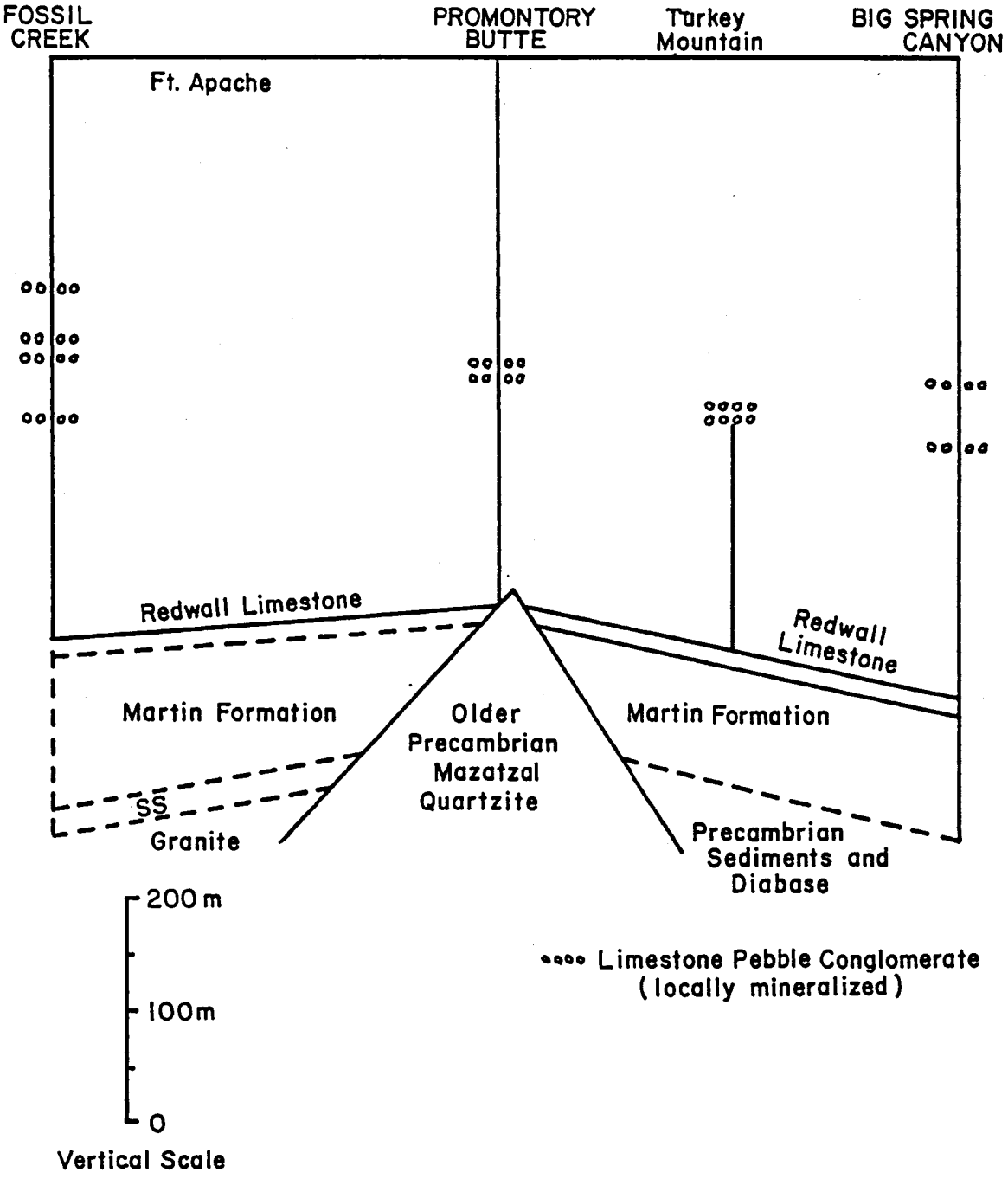

Fig. 2. Stratigraphic Correlation of Mineralized Horizons

Measurements made for this study are shown as solid lines.

thicker in Fossil Creek than elsewhere; the reason for this is not clear. It appears that the sequence between the conglomerates and the Fort Apache is thickening to the east. On the basis of the correlation shown in Fig. 2, the mineralization will be referred to as "strata-bound."

LITHOLOGY

The mineralized localities exhibit a variety of lithologies, including conglomerates, quartz arenites, siltstones, micrites, mudstones, and carbonaceous beds. The thickness and structure within any given lithology is variable. Where exposures permit lateral tracing, most lithologies pinch out over distances on the order of tens to hundreds of meters. There is no definite stratigraphic order in which the various lithologies regularly are found. The sequence is characterized by variability and yet the sequence as a whole can be recognized from place to place, based on the presence of the limestone pebble conglomerates.

Conglomerates

The clasts of the conglomerates, some of which are mineralized, are predominately limestone and dolomite of a wide variety of colors and of pebble and cobble size. Some clasts are larger, up to thirty centimeters. A subordinate number of sandstone, siltstone, and claystone clasts of various colors are present. The matrix of the conglomerates is made up of fine-grained quartz, sand, silt, micrite, and sparry calcite. Most of the conglomerates are matrix supported and most have been dolomitized, in at least one case up to 60 percent. Trace amounts of micas, plagioclase, potassium feldspar, and heavy minerals such as zircon are present. All of the clasts observed could have been derived from units similar to those that occur within the

fifty meters of rock stratigraphically below the conglomerates. A small number of quartzite clasts, as well as some sand and silt, may have been contributed by features such as Pine and Christopher Islands.

Generally, the conglomerates are unstratified, but some units reveal poorly developed bedding. Lenses, up to one meter thick, of quartz arenite are common within the conglomerates. The quartz arenites are commonly planar cross-bedded with sets up to fifteen centimeters thick. The base of the conglomeratic units is an erosional surface where observed. These erosional surfaces show grooves cut into underlying units in some instances. In some locations, rip-up clasts, up to thirty centimeters in longest dimension, of the unit directly below the conglomerates, are found within the conglomerate. Conglomerates are locally found as the basal lithology of a point bar sequence. The point bar sequences grade upward to carbonaceous and/or silty beds.

Evidence of algal activity is found in and with conglomerates at some localities. In Fossil Creek, a stromatolite occurs along the edge of a conglomeratic unit. Some of the clasts within the conglomerate have been surrounded by algal growths. In the field, this feature is exemplified by laminated rims surrounding clasts and, usually, there is a color difference between rim and clast. In thin sections of conglomerates from localities throughout the study area, some clasts were observed to have rims different in color from the interior of the clasts. In some cases, the rims completely encircle (2 dimensions) the clast and in some cases they are found to occur

only part way around the clast. In some cases, the rims show laminations which are sub-parallel to the edge of the clast. These rims may be similar to the algal rims observed in the field or they may be similar to the micrite rims described by Bathurst (1966) which he related to the activity of boring algae. In some instances, conglomerates were observed to contain fragments of algal mats.

Individual conglomerate units attain a maximum thickness of approximately ten meters and are very lensy in two dimensions (channels). Individual lenses can seldom be traced for over ten meters laterally. Often at the lateral termination of a lense another will begin at approximately the same stratigraphic position, and often within ten meters lateral distance. In outcrop, this results in ledge zones, capped by conglomerates, which locally can be traced for kilometers.

Quartz Arenites

In addition to the sandy lenses within the conglomerates, there are also strata of quartz arenite, some of which contain mineralization. The grains in these rocks are almost totally, fine to very fine grained, quartz with only a trace of micas, feldspars, or heavy minerals. The cement of these rocks is sparry calcite. The cement has been partially dolomitized, 0 to 50 percent. Individual units are up to five meters thick. Bedding ranges from very thin laminations to separate beds up to fifteen centimeters thick and is often very irregular. The irregular bedding is the result of primary factors, such as hummocky cross-stratification (Harms et al. 1975), and

secondary factors, such as burrowing organisms. Channel structures are common and planar and trough cross-bedding are found in some instances. Planar cross-bedding is more common than trough. At two localities, structures interpreted as soft sediment deformation have been found closely associated with conglomerates. The contacts of these units vary from place to place; some are sharp lithologic breaks while others are gradational to a different lithology and still others are erosional. Their color ranges from light red 5R 6/6 and moderate reddish-brown 10R 4/6 through pale red purple 5RP 6/2 to gray N6 to N8. The beds can be traced laterally for distances on the order of tens of meters to hundreds of meters.

Siltstones

Siltstone units up to fifteen feet thick are present. Bedding ranges from laminated to massive and is sometimes highly irregular. This irregularity probably results from primary causes, such as flaser structures (Reinack and Wunderlich, 1968), and secondary causes, such as disruption by burrowing organisms or plant roots. The siltstones are almost always highly calcareous and locally are micaceous. The lower contact, where observable, ranges from gradational to sharp. Lenses of quartz arenite are locally found within the siltstone beds. The color of siltstone units ranges from pale reddish-brown 10R 4/6 through grayish red purple 5RP 4/2 to gray N4 to N7. An unusual color phenomenon is locally present within quartz arenite and siltstone beds. Circular to elelliptical patches, five to ten centimeters in diameter, of gray, green, purple, and black are erratically distributed within a

rock of otherwise homogeneous, but different, color. No difference in composition could be observed in hand specimen between the colored patches and the surrounding rock.

Micrites

Sparse gray N7 to black N1 micrite beds are present. In Fossil Creek, these beds contain sparse mineralization. They range in thickness from five to sixty centimeters. Contacts of the micrites with other units are sharp lithologic breaks. Internal structure of these units indicates that they are probably of algal mat origin. The rocks contain numerous fossil fragments (ostracods?). The beds can be traced for distances on the order of meters to tens of meters.

Carbonaceous Beds

Beds from five centimeters to one meter containing a large proportion of carbonaceous (plant) material are locally present. They commonly contain thin laminae of gypsum or halite. These beds are usually associated with siltstones and locally are part of point bar sequences. The beds can be traced laterally for distances of from meters to tens of meters.

Claystone

Locally, claystone beds up to three meters thick are found. They are usually grey N5 to N7, highly calcareous, with very irregular bedding and may be associated with carbonaceous beds. Clay size carbonate is found associated with conglomerates.

ENVIRONMENT OF DEPOSITION

The sediments of the mineralized zone exhibit a variety of structures which relate to their environment of deposition. Channel structures, point bar deposits, cut and fill structures, and rip-up clasts all indicate fluvial processes. These features are well developed in the conglomerates. The soft-sediment deformation in the Quartz Arenites indicates a high rate of sedimentation where over-steepened slopes may develop. The stromatolites indicate intertidal to supratidal environments near large bodies of water, fresh or marine (Davies 1970). Blazey (1971), after studying the fossil flora at Promontory Butte, concluded that some of the species preserved were autochthonous and had grown in a shoreline environment, while other species had grown in the "uplands" and were carried to the site of deposition by sluggish streams. It is suggested that all of the features observed fit well with a shoreline environment of deposition. If this is correct, the unit is time transgressive from northwest to southeast following the retreat of the Pennsylvanian seas.

MINERALIZATION

The mineralization found is varied in both mineralogy and mode of occurrence. Sulfide and oxide copper minerals, sulfides of lead and zinc, and uraninite (?) (UO_2) are present. Whole rock analyses of selected grab samples revealed silver up to half an ounce per ton, nickel values up to 65 ppm, minor molybdenum and traces of gold. Overall, the mineralization is very restricted in a stratigraphic sense, but is widely though discontinuously distributed in a lateral sense.

At Fossil Creek, conglomerates contain pyrite, malachite, chalcopyrite, bornite, chalcocite, and covellite. These minerals occur as blebs in pebbles and matrix. Some quartz arenites contain azurite and malachite, pyrite, chalcocite, and covellite. These occur as nodules and as cavity fillings. Micrites have been found to contain hematite, pyrite, marcasite, chalcocite, and covellite, occurring as blebs within the rock along bedding planes and, in some cases, fractures that follow bedding planes. Carbonaceous units contain azurite and malachite as thin laminae within beds. The different types of mineralization described above are found to occur at various geographic locations in Fossil Creek. At any given locality, the mineralization can be traced laterally for a distance of meters to tens of meters.

Mineralization at Promontory Butte is found predominately in conglomerates and quartz arenites, although some malachite is found in one thin carbonaceous layer. Conglomerates contain uraninite, pyrite,

chalcopyrite, bornite, chalcocite, digenite (?), covellite, sphalerite, galena, malachite, azurite, and marcasite, occurring as blebs in pebbles and matrix, surrounding and replacing pebbles, and in veinlets with secondary calcite. Often these calcite veins will be in and around the remains of carbonaceous (plant) material, in which case the mineralization tends to be more highly concentrated around the carbonaceous material. The mineralized quartz arenites occur as lenses within the mineralized conglomerates and contain the same ore mineralogy as the conglomerates. The mode of occurrence of the ore minerals is also the same. The mineralization has been exposed by two major excavations made into the front of the Butte; at each location the mineralization can be traced laterally on the order of tens of meters.

The mineralization at Turkey Mountain is associated with a conglomeratic bed and quartz arenite bed. Both beds contain azurite and malachite as well as pyrite, chalcocite, and covellite. The sulfides in the conglomerate occur as blebs in pebbles and matrix, and as ellipsoidal masses, up to one inch in longest dimension, with the longest dimension being within the plane of bedding. Azurite and malachite, in both units, occur as circular to elliptical masses on bedding planes and as open space fillings in both the conglomerate and the arenite. The sulfides in the quartz arenite occur as irregular masses which tend to follow bedding and cross-bedding.

Four silver analyses in excess of 8 ppm have been obtained from whole rock grab samples of conglomerates, three from Promontory Butte and one from Turkey Mountain. Uranium analyses were obtained for rocks

from all three localities. Uranium values in excess of 100 ppm were obtained for several samples from Promontory Butte, two analyses in excess of 50 ppm were obtained for samples from Fossil Creek and values for Turkey Mountain ranged from 7 to 28 ppm.

PETROGRAPHY

Approximately thirty-five polished surfaces were studied with the petrographic microscope. On eleven of the polished surfaces, pyrite was the only sulfide observable. On the remaining twenty-four, at least one copper sulfide is present and these samples exhibit significant and interpretable textural relationships.

Some of the observable textures show what appears to be straightforward replacement, i.e., Fig. 3. This suggests a paragenetic sequence of pyrite being replaced by chalcocite, which in turn alters to covellite. This sequence is commonly present.

Other textural relationships suggest that pyrite was replaced by bornite, bornite was replaced by chalcopyrite and chalcocite, and bornite and chalcopyrite were replaced by chalcocite.

Some textures are much less easily interpreted. Textures similar to the tubercle replacement textures of Bastin (1950) have been found. Tubercle textures involve several different sulfide minerals surrounding and replacing carbonate pebbles. Pyrite, bornite, chalcocite, and covellite are found in masses surrounding and replacing carbonate pebbles in conglomerates at Promontory Butte (Fig. 4). It is important to note that it is impossible to determine a paragenetic sequence from Fig. 4. There is a suggestion that the chalcocite and covellite are later than the pyrite and bornite because they occur in the outer portion of the mass.

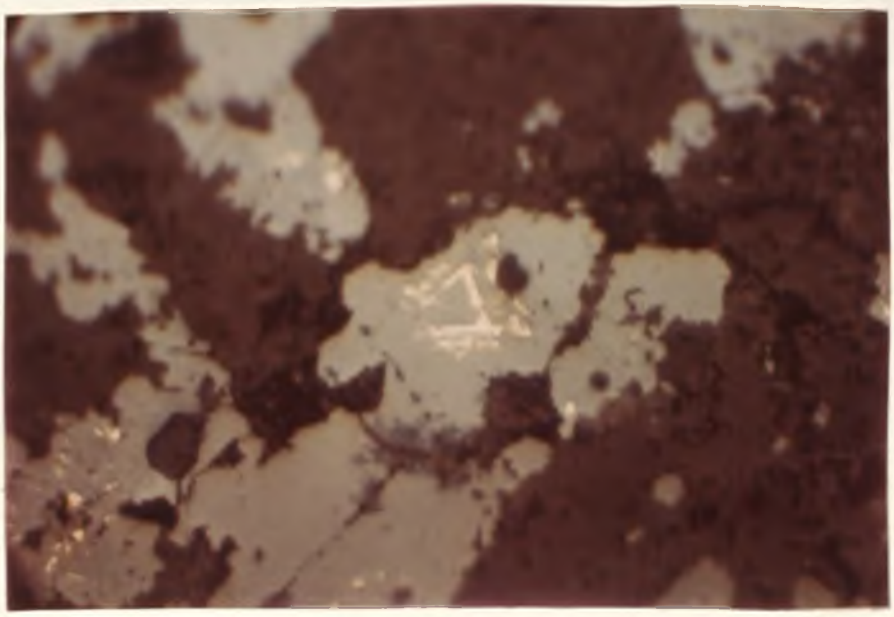

Fig. 3. Chalcocite Replacing Pyrite, with Minor Covellite
Field of view is 550 microns wide.

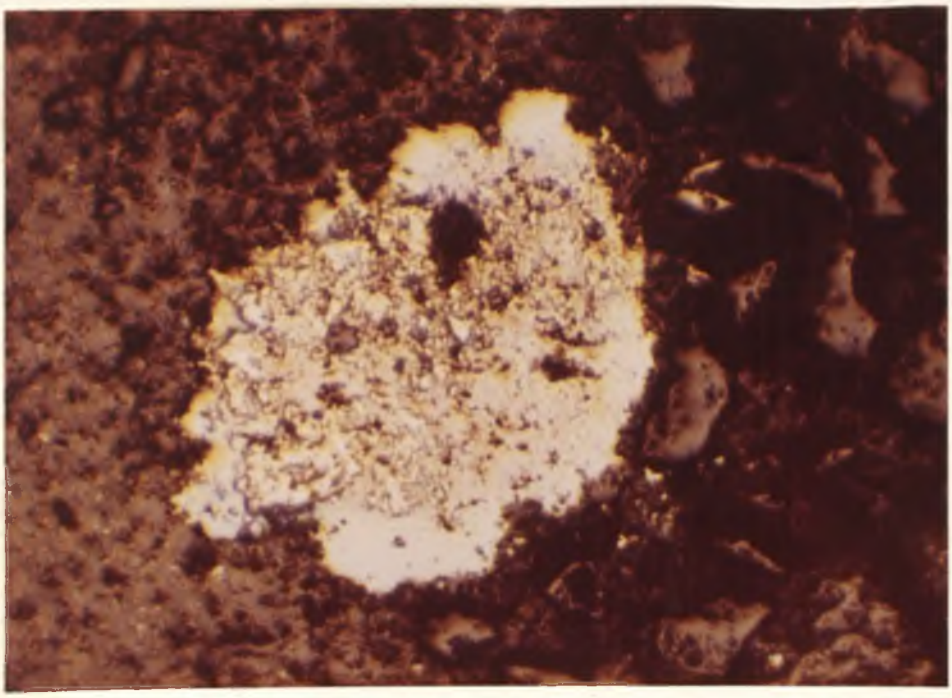

Fig. 4. Bornite + Pyrite Surrounded by Chalcocite

Field of view is 550 microns wide.

Some textures may indicate replacement, but which mineral is replacing the other is unclear, i.e., Fig. 4. This texture may also indicate coprecipitation. Similar textures have been observed involving bornite and pyrite or chalcocite ± chalcopyrite. These textures may indicate replacement, coprecipitation, or both. Fig. 5 shows an interesting relationship. Bornite may be interpreted as replacing chalcocite, and chalcopyrite appears to be replacing both.

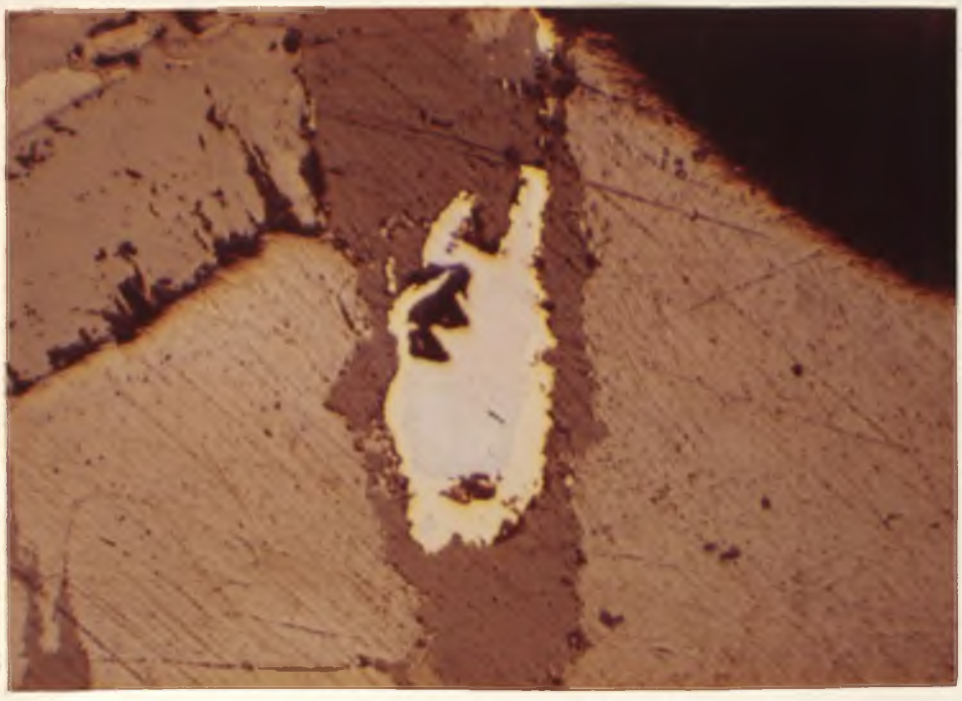

Fig. 5. Bornite + Chalcocite Surrounded by Chalcopyrite

Field of view is 550 microns wide.

GEOCHEMISTRY

At all three mineralized localities, hand sample size specimens were collected and analyzed for copper, uranium, and vanadium content. A total of eight stratigraphic sections were measured in the mineralized interval. A hand sample was collected from each unit that was measured and described. A systematic grid pattern was sampled at one face at the Promontory Butte locality (Jones 1977). Several additional hand samples were collected of mineralized rocks for special study.

Plots were made of copper, uranium, and vanadium content vs. position in stratigraphic column for the five columns measured in Fossil Creek. Fig. 6 shows both the metal content in ppm and the lithology of the unit from which the sample was collected. The clearest association to be seen from these graphs is between high metal content, especially copper, and organic material. There is also a suggestion of higher metal content associated with the finer-grained rocks.

Metal ratios were also investigated for the Fossil Creek specimens. Cu/V, Cu/U, V/U, and Cu/(U + V) were investigated. No consistent relationships were found. In some sections, Cu/U and V/U behave sympathetically and in others they behave antithetically. In one section, Cu/V, Cu/U, and U/V are high in sandstones and low in siltstones and in another section the exact opposite relationship is found.

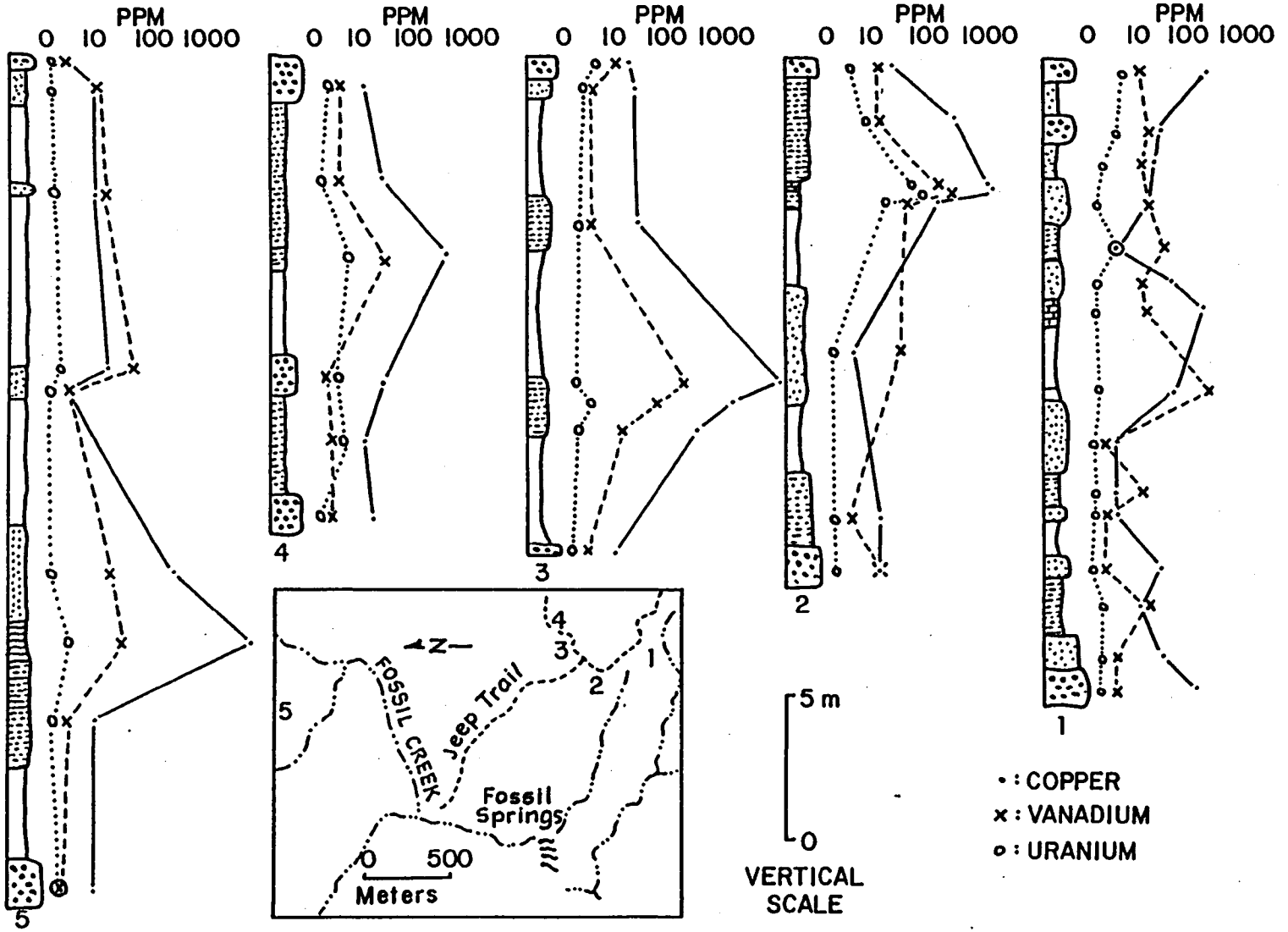

Fig. 6. Measured Sections in Fossil Creek

Geochem analyses, in parts per million. For lithologic descriptions see Appendix A.

CARBONACEOUS MATERIAL

Perhaps the most striking characteristic of the mineralization is its close spatial association with carbonaceous material. This association manifests itself at any scale of observation, from the study area as a whole, through outcrop and hand sample to microscopic scale. Within the study area, the three mineralized localities are also the sites of the largest known concentrations of carbonaceous material. Sulfide mineralization has not been found without closely associated carbonaceous material.

There are two types of carbonaceous material preserved. One type consists of the carbonized remains of land plants, while the other type is characterized by black fetid limestone with algal structures. The plant remains occur as crusts of black carbonized material, up to 5 mm thick, on bedding planes. Much of this black carbonized material looks remarkably like the bark from a tree. Pieces with lengths and widths of several tens of centimeters have been found.

Black fetid micrites up to sixty centimeters thick were found in Fossil Creek. In this section, these rocks exhibit algal structures. Black limestone pebbles, thought to have an origin similar to the black fetid micrite, are present in conglomerates at all three localities. Fragments of algal mats, up to 5 mm thick, are preserved in conglomerates at all three localities. The algal mat fragments are best developed at the Turkey Mountain locality. At this locality, examples up to several centimeters long have been found on bedding planes.

At Fossil Creek, there are several carbonaceous beds which often contain azurite and malachite. Copper sulfides, as well as azurite and malachite, have been observed in siltstones containing carbonaceous material. At Promontory Butte, mineralization is found in conglomerates and quartz arenites which contain plant remains. At Turkey Mountain, the conglomerate bed and the quartz arenite bed which contain carbonaceous remains also contain copper sulfides in addition to azurite and malachite.

In hand specimen mineralization is generally concentrated around carbonaceous remains. At Promontory Butte, uranium and some sulfide mineralization is found in and around the carbonized plant material. At Fossil Creek, copper sulfides and azurite and malachite are found in and around carbonized plant material and in black micrite units. At the Turkey Mountain locality, quartz arenite has been found with carbonaceous material which follows cross-bedding. Pyrite, chalcocite, and covellite are associated with this carbonaceous material. In the conglomeratic unit at Turkey Mountain, mineralization tends to be in the same samples contain fragments of algal mats. At Fossil Creek, a nodule was found which contained in its center a texture which is interpreted as having cellular (wood) structure; the cells are filled with marcasite and chalcocite and the cell walls are partially replaced by chalcocite and covellite (Fig. 7).

Fig. 7. Cellular (Wood) Structure, with Marcasite Filling Cells

Field of view is 550 microns wide.

SULFIDE GENESIS

It has been suggested that the sediments under discussion were deposited as part of the shoreline sequence developed as the Pennsylvanian seas regressed from central Arizona. Modern shoreline environments have been studied extensively. Love (1969) and Swanson, Love, and Frost 1972) have paid particular attention to the metal contents of these sediments. Love has found amorphous FeS_2 within one meter of the surface in some modern environments. The FeS_2 is found where organic material creates the chemical conditions necessary for the growth of sulfur reducing bacteria. These bacteria produce reduced sulfur in the form of H_2S gas. The H_2S gas reacts with solutions that pass through the sediments and removes iron from the solution to precipitate FeS_2.

Analogy with modern environments would suggest that it is no accident that the sulfide mineralization under consideration is closely associated with carbonaceous material. Copper sulfides, however, are notable for their reported absence in modern sedimentary environments. This leads to the question of when the copper was introduced into the system under study.

The actual time of formation of the copper sulfides is impossible to determine, but there are suggestions that at least some of them formed prior to lithification of the rock. In some conglomerates, sulfide minerals and lime mud are found filling irregularities along the edge of carbonate clasts. If these irregularities result from the dissolution of calcite during the mineralization event, then lime mud

must have been sufficiently mobile to move into the cavities, i.e., lithification was not complete. The preservation of the cellular texture previously described (Fig. 7) shows that something filled the cells and replaced the walls before sufficient sediment had accumulated above it to crush the cells, as has been suggested at Corocoro in Bolivia (Entwistle and Gouin 1955). The tubercle textures (Fig. 4) indicate a high degree of porosity in the sediments, since fluids must have been able to surround the carbonate pebbles, to deposit the sulfides as seen. Some sulfide blebs are seen surrounded by carbonate and with no evidence of fractures leading to them. The above evidence is thought to suggest that at least some mineralization occurred prior to lithification.

Another interesting question is where the copper came from, or perhaps more importantly, what was the chemistry of the ore forming solution? It may be that these two questions are intimately interconnected and that the answer to one may lead to the answer to the other. An igneous source for the mineralization solution is thought to be very unlikely. There is no evidence for Phanerozoic intrusive activity in the area. The closest is the Laramide intrusive activity associated with the prophyry copper deposits at Globe-Miami. Tertiary volcanics and their associated feeder dikes found locally along the Tonto Rim, show no consistent relationship to mineralization. Groundwater is one possibility as a mineralizing solution and the other possibility is an evaporite brine that might have been associated with the overlying redbeds. Evaporite processes were beginning in the general region in

Lower Supai time, as evidenced by the occurrence of gypsum and anhydrite. These processes became fully developed in Upper Supai time, with the deposition of halite and some sylvite in the Holbrook basin to the northeast.

CALCULATIONS

The geologic evidence suggests that the mineralizing solutions were either groundwater or brines. Thermodynamic calculations were employed to test the two hypotheses. Calculations were made for two distinct solutions. Several analyses of groundwater from the area of this study were averaged to give one solution. The second starting solution composition was obtained by averaging several analyses for brines reported by Carpenter, Trout, and Pickett (1974). The stratigraphy of the basin where Carpenter's brines were collected is very similar to the stratigraphy of the region under study. It is suggested that brines that formed in the region during Permian time were probably very similar in composition to the central Mississippi brines reported by Carpenter and others.

The analyses obtained from the literature were incomplete. Values for the molality of $S^{=}$ and total Cu were needed for each solution. The value for the molality of $S^{=}$ was obtained by determining an fO_2 value suitable for groundwater and setting the $m_{SO_4^{=}}/m_{S^{=}}$ ratio equal to the value needed to obtain this fO_2. The fO_2 value was obtained from a modified version of Fig. 11.2 of Garrels and Christ (1965). Log fO_2 was set to approximately -65.

One of the parameters to be obtained from the calculations was the mass of copper introduced into the rock during reaction with the solutions. For this reason, the maximum amount of copper possible was put into each solution. The m_{Cu} in each solution was therefore set

just below the amount needed to equilibrate with the first copper mineral. The initial molality of copper assumed for the solution may have resulted in calculations predicting precipitation of more copper per kilogram of solution than actually occurred during the natural processes. Nevertheless, it seems to be the most reasonable assumption to test the two hypotheses.

Calculations were made using the PATH program of Helgeson et al. (1970), as modified by Knight (1976). The program performs the thermodynamic calculations involved in equilibrating one kilogram of solution, of a given chemical composition, with given reactant minerals. Changes in solution chemistry due to the incremental addition of reactant minerals are calculated. As the reactant minerals are dissolved, the concentration of the ions in the solution increases until the point is reached where some mineral phase becomes saturated with respect to the solution and precipitates. As reactant minerals continue to be added to the solution, the program calculates the mass of product phase produced. A sequence of product minerals may be produced as the solution sequentially equilibrates with additional mineral phases. As the reaction continues toward equilibration, mineral phases produced early in the reaction may be destroyed later in the reaction as the solution chemistry changes. Dissolution of incremental amounts of reactant minerals continues until the solution is in equilibrium with all reactant phases.

The reactant minerals used, with the relative proportions in which they were added, were calcite (60 percent), quartz (35 percent),

and pyrite (5 percent). It is believed that this adequately represents the initial mineralogical composition of the rocks (or sediments) prior to the time that the copper sulfides were introduced.

The consequences of the two reactions are shown on Figs. 8 and 9. The successive sulfide phases generated during each reaction have been shown on activity-activity diagrams (Figs. 10 and 11). a_{Cu^+}/a_{H^+} and $a_{Fe^{++}}/a_{H^+}{}^2$ have been chosen for the axis' of these diagrams because it is felt that these will best illustrate what is happening in the system. During the groundwater reaction, the Log A $(SO_4^=)$ $(H^+)^2$ shows little variation. For this reason, the Log A $(SO_4^=)$ $(H^+)^2$ was fixed to generate the activity-activity diagram (Fig. 11). During the brine reaction the Log A $(S^=)$ $(H^+)^2$ varied less than the Log A $(SO_4^=)$ $(H^+)^2$. Consequently, Log A $(S^=)$ $(H^+)^2$ was fixed at an average value to generate Fig. 12.

Reaction of the Quartz + Calcite + Pyrite rock with the groundwater solution leads first to the precipitation of chalcocite at point 1 (Fig. 10). Cu^+ precipitates from solution as the solution composition is driven across the chalcocite field, causing the replacement of pyrite by chalcocite. At point 2, the reaction crosses the chalcocite-bornite phase boundary and begins to destroy chalcocite and produce bornite. Continued reaction drives the solution composition across the bornite field causing bornite to completely replace the chalcocite that was previously produced and to partially replace the pyrite that was initially present. At point 3, the reaction reaches the pyrite-bornite phase boundary and subsequently moves along this boundary, resulting in

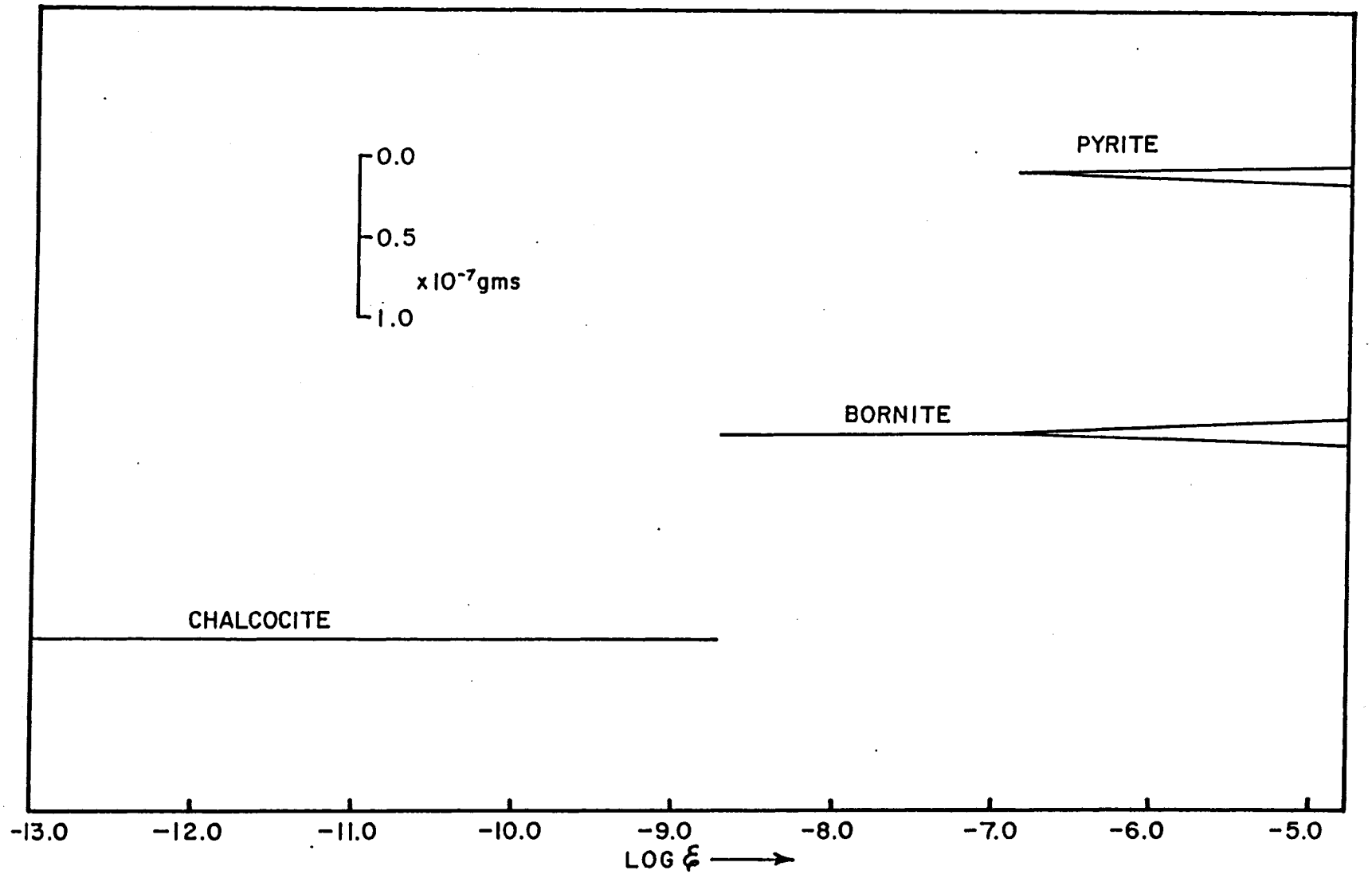

Fig. 8. Phases Produced during Groundwater Reaction

Graph shows reaction progress vs. mass abundance of phases produced.

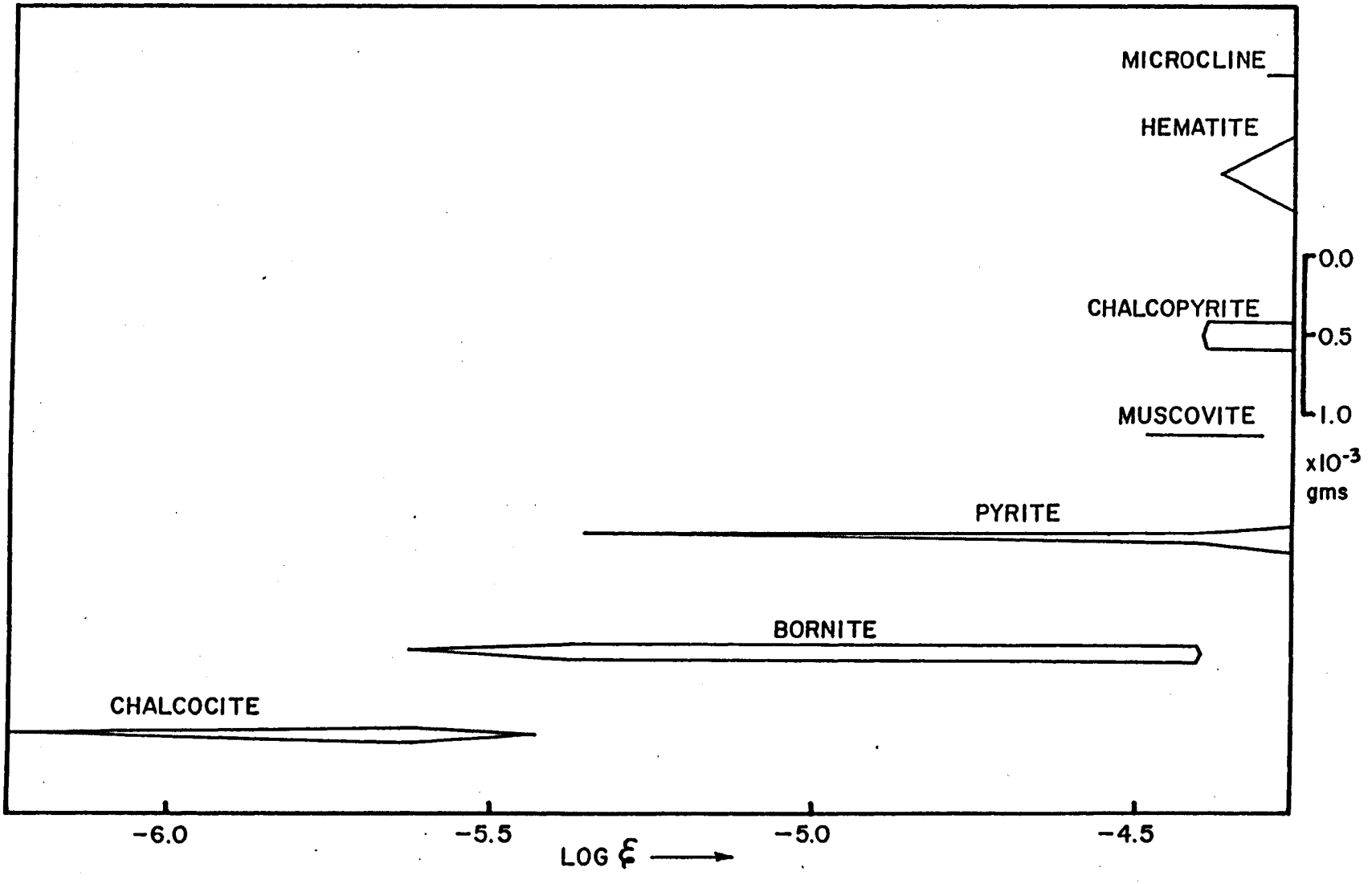

Fig. 9. Phases Produced during Brine Reaction

Graph shows reaction progress vs. mass abundance of phases produced.

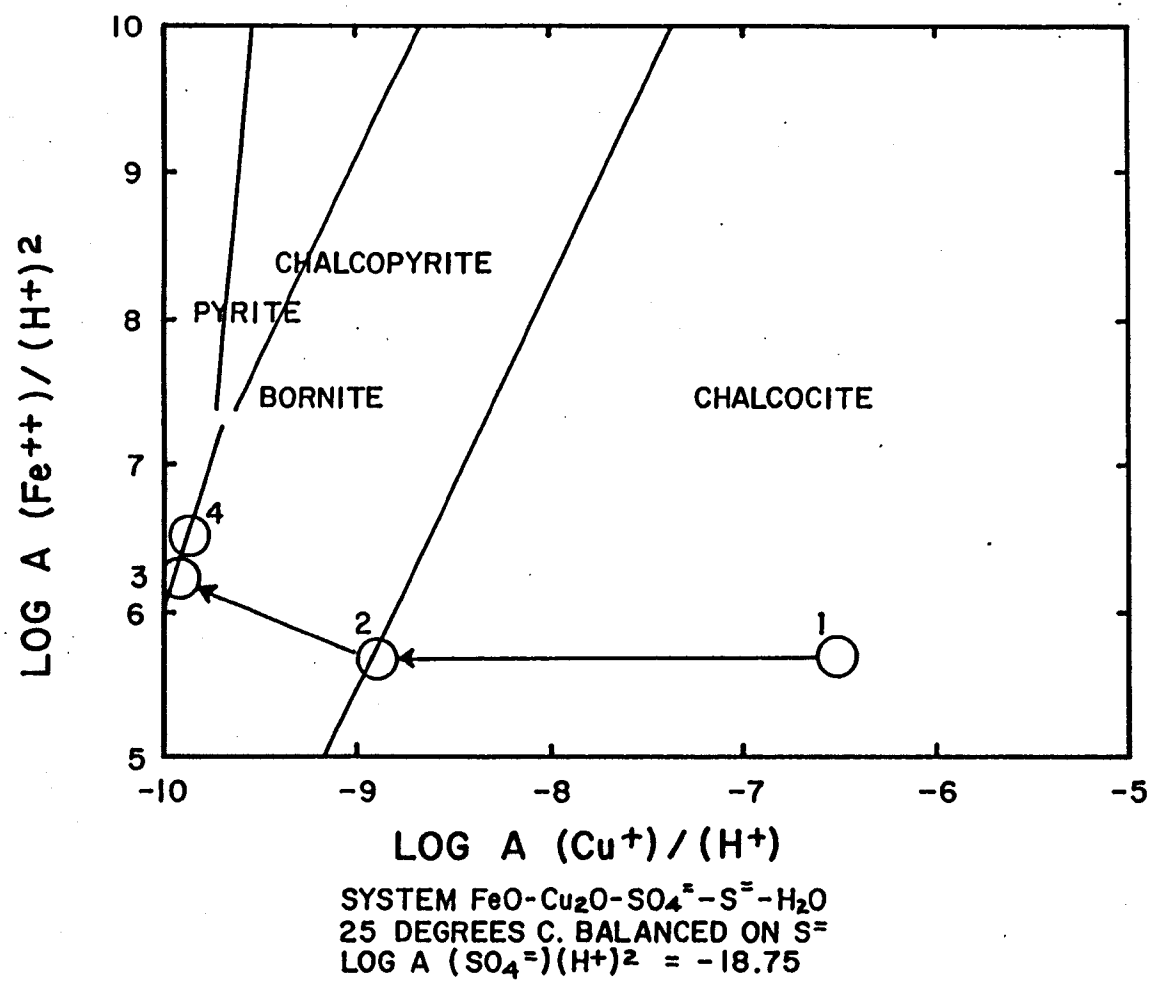

Fig. 10. Chemical Variations during Groundwater Reaction

Reaction between groundwater and calcite + quartz + pyrite rock. Diagram shows successive phases solution equilibrated with.

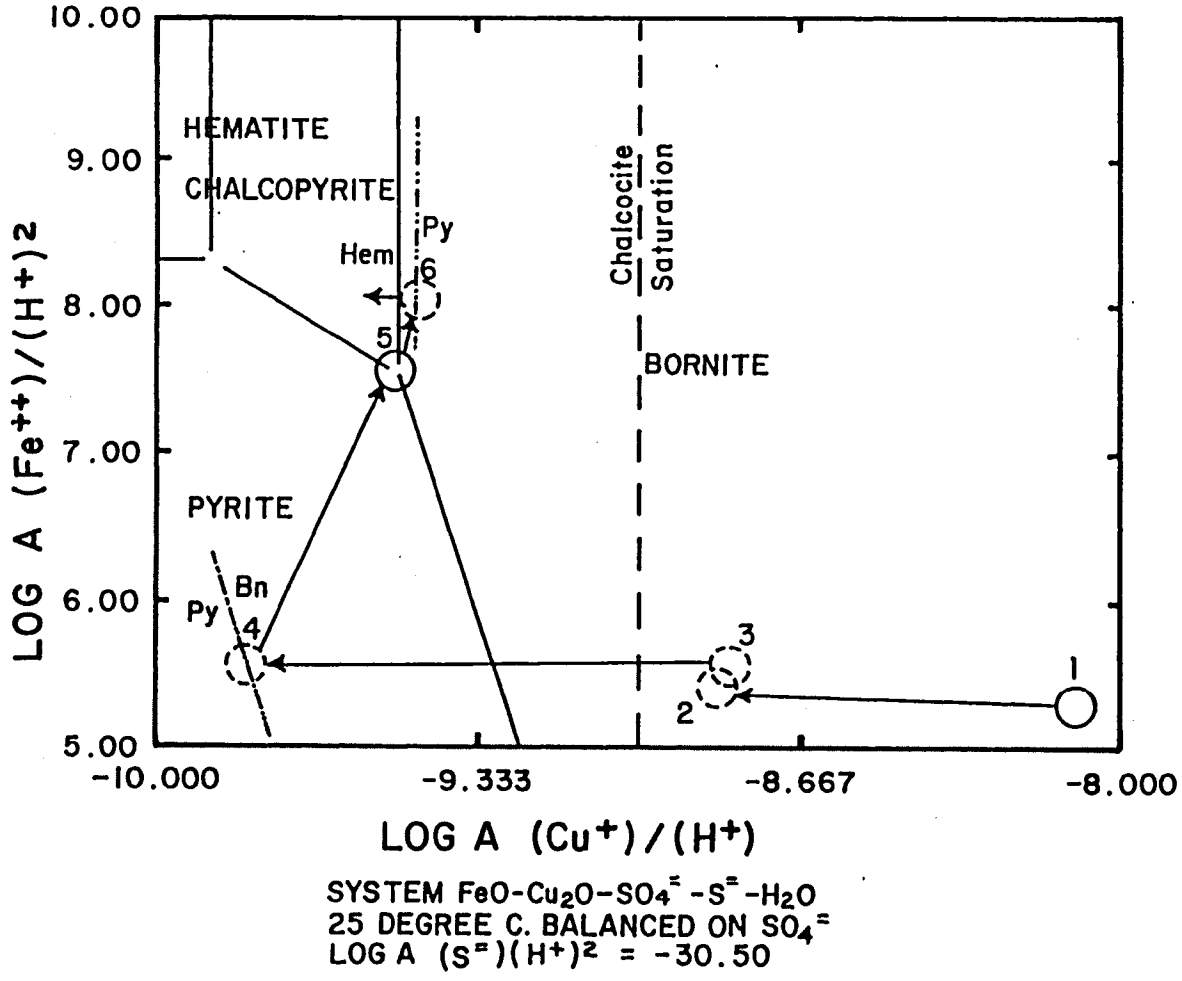

Fig. 11. Chemical Variations during Brine Reaction

Diagram shows successive phases solution equilibrated with. Dashed circles represent points projected onto diagram. Dotted lines represent phase boundaries projected onto diagram.

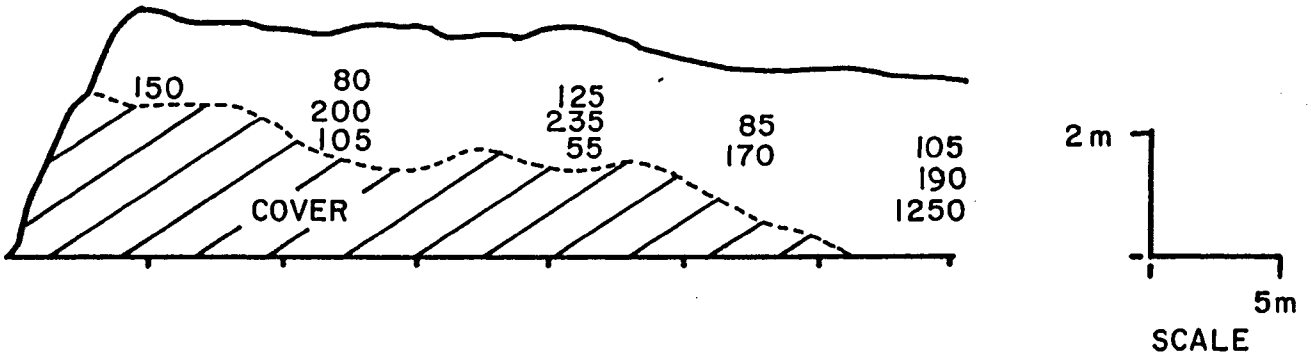

Fig. 12. Detail Sampling at Promontory Butte

Concentrations of copper at sample locations shown in parts per million (modified from Jones 1977).

the co-precipitation of pyrite and bornite. At point 4 overall equilibrium is established between the aqueous solution and the minerals in the rock.

Phases produced during the brine reaction are shown on Fig. 11. The interpretation of Fig. 11 is more difficult than Fig. 10 because the solution composition moves in and out of the plane of the diagram. To generate the diagram shown on Fig. 11, the Log A $(S^{=})$ $(H^{+})^{2}$ was fixed but during the reaction it was hot fixed. One such example is the point where the reaction reaches the pyrite-bornite phase boundary. This point does not correspond exactly to the pyrite-bornite on the diagram. Point 4, for instance, is on the pyrite-bornite phase boundary but not in the plane of the diagram.

Reaction of the Quartz + Calcite + Pyrite rock with the brine solution leads first to the precipitation of chalcocite at point 1 (Fig. 11). Continued reaction drives the solution composition across the chalcocite field resulting in chalcocite replacing pyrite. At point 2 the bornite stability field is reached and bornite and chalcocite are both precipitated as the solution composition moves to point 3. Continued reaction drives the solution composition across the bornite stability field resulting in bornite replacing all of the chalcocite previously produced and some pyrite. At point 4 the pyrite stability field is reached and pyrite and bornite are both precipitated as the solution composition is driven to point 5. At point 5 the chalcopyrite stability field is reached and as solution composition moves from point 5 to point 6, pyrite and chalcopyrite are precipitated

and chalcopyrite replaces all of the previously deposited bornite. At point 6 the hematite stability field is reached and pyrite, chalcopyrite and hematite are precipitated until overall equilibrium is reached between the aqueous solution and minerals in the rock. During the reaction, trace amounts of muscovite and microcline are produced.

DISCUSSION

In interpreting the results of the calculations, two questions need to be considered: 1) Do the assumptions made in developing the mathematical model adequately describe the geologic situation? and 2) If they do, what conclusions can be drawn from them?

Figs. 3, 4, and 6 all display textures which are predicted at different stages of reaction progress by the calculations. Perhaps the most notable deviation from the thermodynamic predictions is the presence of covellite. Covellite was not a phase whose presence was predicted by any of the calculations. The covellite present is always found intimately related to chalcocite and it may be that chalcocite was the original phase deposited and that the covellite is a late stage alteration product. There is also a suggestion in some of the textures observed, such as Fig. 4, that chalcocite is replacing bornite, which was not predicted.

The fact that the geometric interpretation of some textures are inconsistent with calculations is an interesting problem. One interesting possibility involves the assumed concentration of copper in the solution. The concentration may have been less than that assumed. A lower concentration of copper could result in the solution initially equilibrating with a different phase, i.e., pyrite or bornite. Hydrogen ion consumption, due to the dissolution of calcite, could drive the solution through the bornite field and into equilibration with chalcocite.

There is, therefore, a close, though not perfect, correspondence between observed and predicted textures in the sulfides. It is suggested that the textures observed represent different stages of the reaction path. It appears that overall equilibrium was reached at different stages along the reaction path in different rocks and in different parts of the same rock. Perhaps lithification of the rock terminated the reactions by eliminating the contact between the sulfide minerals and the solution. Lithification would be a relatively early event, since Pleistocene limestones are completely lithified.

It is suggested from this study, therefore, that the thermodynamic calculations do provide a reasonable model for the geologic processes which deposited the sulfides. One interesting result is that 6.36×10^{-5} grams of copper/kg H_2O could have been introduced into the rock by the brine solution and 1.16×10^{-8} grams of copper/kg H_2O could have been introduced into the rock by groundwater. At Promontory Butte, a sulfide-bearing unit is exposed whose dimensions are at least 2 m x 40 m x 150 m, or 12,000 m^3. A portion of this unit has been sampled on a grid pattern (Fig. 12). The unit averages 222 ppm copper. If a density of 2.7 is assumed for the rock, then approximately 7200 grams of copper are present in the rock volume discussed above. 1.13×10^8 kilograms of brine would be required to introduce this much copper into the rock and 6.20×10^{11} kilograms of groundwater would be needed.

The amount of time involved in the deposition of the sulfides is an intriguing question. A simple Darcy's law analysis was done for

this situation using equation (1):

$$\vec{q} = \frac{-k\rho}{\gamma} \quad \vec{g} \frac{\Delta h}{l} \tag{1}$$

where $\vec{q}$ = mass flux in gm/cm^2-sec, k = permeability in cm^2, ρ = density of H_2O in gm/cm^3, γ = viscosity in cm^2/sec, $\vec{g}$ = acceleration due to gravity in cm/sec^2, and $\Delta h/l$ = gradient on the water table.

Scherer (1976) has measured the porosity and permeability of Holocene and Pleistocene corals. A value of 8.0×10^{-9} cm^2, which Scherer's work would indicate was higher than average, was picked. A gradient of 10 percent was selected for the water table. The values for ρ, γ, and $\vec{g}$ were taken from standard tables. A value of 1.01×10^{-8} gm/cm^2-sec was obtained for the brine and of 7.84×10^{-9} gm/cm^2-sec for groundwater. A value for time was obtained by dividing the mass of mineralizing fluid by the mass flux times the cross-sectional area through which the solution flowed. Calculations suggest that it would take 4.44×10^5 years for the brine to mineralize this volume of rock while it would take groundwater 3.18×10^9 years.

The calculations clearly indicate that the brine is the more likely mineralizer in these rocks, which are approximately 3.0×10^8 years old. It has been suggested that at least some of the mineralization occurred prior to lithification of the rock. In this light, even the time required for mineralization by the brine seems long, since Pleistocene carbonate rocks are lithified. It seems reasonable to expect some degree of mixing between brines and less saline groundwaters. The time calculations suggest that this amount of mixing was slight.

CONCLUSIONS

The sulfide mineralization in the lower portion of the Supai Formation along the Mogollon Rim is best described as stratabound. Textural relationships suggest that chalcocite and bornite replaced pyrite, bornite was replaced by chalcopyrite and chalcocite, and bornite and chalcopyrite replaced chalcocite. Masses of bornite and pyrite or chalcocite ± chalcopyrite represent co-precipitation and, possibly, some replacement. The mode of occurrence of the sulfides suggests that at least some of the mineralization occurred prior to lithification.

Groundwater or brines have been considered as possible mineralizing solutions. These hypotheses were tested through the use of computer modelling. 6.36×10^{-5} grams of Cu/kg of H_2O could have been introduced into the rock by brines and 1.16×10^{-8} grams of Cu/kg of H_2O could have been introduced by groundwater. The mineralization exposed in one cut at Promontory Butte could have been produced by 1.18×10^{8} liters of brine or by 6.20×10^{11} liters of groundwater. An analysis employing Darcy's law suggests that the brine could complete mineralization in 4.44×10^{5} years while it would take groundwater 3.18×10^{9} years, suggesting that the brine is the more likely mineralizer.

APPENDIX A

MEASURED STRATIGRAPHIC SECTIONS

Fossil Creek Canyon

Access: State 87 to Strawberry; west on Fossil Creek--Camp Verde road to jeep trail at elev. 5640 shown of Strawberry quadrangle, 7.5' series. Exposures in cuts at elev. 5120 below and west to northwest of Nash Point. Also exposures in cuts 1/2 mile north of Fossil Creek 1/8-1/4 mile east of Mud Tanks Draw at elev. 4640-80. Locations of measured sections shown on Fig. 7.

Top of Section 1

Unit no.	Description	Unit Thickness (meters)	Cumulative Thickness (meters)
17	Conglomerate, grayish-brown (5YR 4/1), micrite and very fine grained quartz arenite clasts, .25 to 5 cm, matrix-micrite and fine quartz sand, base in erosional contact	(.74)	22.64
16	Conglomerate, light-brown (10YR 6/2), micrite and very fine grained quartz arenite clasts, .25 to 5 cm, matrix-micrite and fine quartz sand, base is erosional contact	(1.17)	21.90
15	Conglomerate, grayish brown (5YR 4/1), micrite and very fine grained quartz arenite clasts, .25 to 5 cm, matrix-micrite and fine quartz sand, base is erosional contact	(1.02)	20.73
14	Quartz arenite, gray (N7), very fine grained, laminated to thin bedded, calcareous cement, gradational to unit 13	(1.22)	19.71

Unit no.	Description	Unit Thickness (meters)	Cumulative Thickness (meters)
13	Quartz arenite, gray (N6), with circular to elliptical color patches near base, grades upward to all purple (5RP 6/2), very fine grained, irregular bedding, .25 to 20 cm, calcareous cement, basal contact probably erosional	(1.68)	18.49
12	Siltstone, dark gray (N5), dominantly quartz with minor mica and black (carbonaceous ?) material, laminated to thin bedded, calcareous cement, gradational to unit 11	(1.24)	16.81
11	Quartz arenite, grayish white (N8), very fine grained quartz, irregular patches of limonite and black (carbonaceous ?) material, irregular bedding, .25 to 2.5 cm, calcareous cement, sharp contact with unit 10	(1.45)	15.57
10	Micrite, dark gray (N4), minor quartz silt, limonite staining near base, irregular bedding, .25 to 7 cm . . .	(.76)	14.12
9	Covered internal-carbonaceous horizon approximately 60 cm from base was sampled for geochem	(2.74)	13.36
8	Subarkose, gray (N7) with circular to elliptical patches of purple near base, grades upward to entirely purple (5RP 4/2), very fine grained with finer grained partings, 5 to 10 cm, laminated to thin-bedded, sharp contact with unit 7	(2.44)	10.62
7	Siltstone, gray (N6), laminated to thin-bedded, calcareous cement, sharp contact with unit 6	(1.19)	8.18
6	Subarkose, gray (N7), very fine grained, irregular bedding, laminated to 15 cm, calcareous cement	(.46)	6.99

Unit no.	Description	Unit Thickness (meters)	Cumulative Thickness (meters)
5	Covered interval	(1.30)	6.53
4	Subarkose, gray (N7) very fine grained, irregular bedding, 5 to 20 cm, calcareous cement, sharp contact with unit 3	(.71)	5.23
3	Siltstone, gray (N6), massive bedding, calcareous cement, gradational contact with unit 2	(2.03)	4.52
2	Quartz arenite, gray (N6), very fine grained with black (carbonaceous ?) material on fractures and within laminae, irregular bedding, .25 to 10 cm, calcareous cement, sharp contact with unit 1	(1.17)	2.49
1	Conglomerate, gray (N7), micrite and fine grained quartz arenite clasts, matrix, micrite and fine grained quartz sand, erosional contact with unit below showing flutes and grooves	(1.32)	1.32

Base of Section 1

Top of Section 2

8	Conglomerate, gray (N7), micrite and fine grained quartz arenite clasts, .25 to 10 cm, matrix-micrite and fine grained quartz sand, erosional contact with unit 7	(.69)	18.19
7	Siltstone, gray (N7), claystone partings, 5 to 15 cm, irregular bedding, 10 to 60 cm, calcareous cement, contains malachite near base, erosional (?) contact with unit 6	(3.66)	17.50

Unit no.	Description	Unit Thickness (meters)	Cumulative Thickness (meters)
6	Siltstone, gray (N7), abundant limonite staining, contains two carbonaceous horizons, 15 cm thick, near top which were sampled for geochem, irregular bedding, siliceous cement	(.89)	13.84
5	Covered interval	(2.74)	12.95
4	Quartz arenite, purple (5RP 6/2), fine grained with very fine grained partings, 5 to 10 cm, irregular bedding, .5 to 13 cm, calcareous cement	(4.22)	10.21
3	Covered interval	(2.36)	5.99
2	Siltstone, gray (N5), micaceous and lithic fragments in upper 30 cm, laminated to thin bedded, calcareous cement, sharp contact with unit 1 .	(2.13)	3.63
1	Conglomerate, gray (N6), micrite and fine grained quartz arenite clasts, .25 to 5 cm, matrix-micrite and fine grained quartz sand	(1.50)	1.50

Base of Section 2

Top of Section 3

8	Conglomerate, gray (N6), micrite and fine grained quartz arenite clasts, .25 to 5 cm, matrix-micrite and fine quartz sand, erosional contact with unit 7	(.81)	17.96
7	Quartz arenite, gray (N7), very fine grained, laminated to thin-bedded, siliceous cement	(.64)	17.15
6	Covered interval	(3.43)	16.51

Unit no.	Description	Unit Thickness (meters)	Cumulative Thickness (meters)
5	Siltstone, purple (5RP 4/2) micaceous, contains circular to elliptical patches of black, same composition, contains 7.5 to 10 cm layer of green, finer grained, not micaceous, irregular bedding, .25 to 90 cm, calcareous cement	(1.98)	13.08
4	Covered interval.	(4.27)	11.10
3	Siltstone, gray (N6), limonite staining prevalent, upper portion contains two carbonaceous horizons which were sampled for geochem, lower horizon is 7.5 cm, upper horizon 15 cm thick, separated by 76 cm, upper horizon contains visible malachite, undulatory black micrite bed, 10 cm thick, above upper carbonaceous seam, unit is thin-bedded with calcareous cement. .	(2.13)	6.83
2	Covered interval.	(4.37)	4.70
1	Conglomerate, gray (N5), micrite and fine grained quartz arenite clasts, .25 to 5 cm, matrix-micrite and fine quartz sand, unit discontinuous . . .	(.33)	.33

Base of Section 3

Top of Section 4

7	Conglomerate, gray (N6) micrite and fine grained quartz arenite clasts, .25 to 5 cm, matrix-micrite and fine quartz sand, erosional contact with unit 6.	(1.57)	16.70

Unit no.	Description	Unit Thickness (meters)	Cumulative Thickness (meters)
6.	Siltstone, purple (5RP 4/2) to reddish-brown (10R 4/6), contains circular to elliptical patches of black, same composition, unit becomes more reddish-brown and contains elliptical patches of green near top, same composition, irregular bedding, .25 to 10 cm, calcareous cement, gradational to unit 5	(4.80)	15.13
5	Siltstone, dark gray (N4), limonite staining common, minor malachite, irregular bedding, .25 to 2.5 cm, calcareous cement	(1.14)	10.33
4	Covered interval	(2.97)	9.19
3	Same as Unit 1	(1.37)	6.22
2	Siltstone, light green (5BG 7/2) and purple (5P 4/2), mostly green near base, mostly purple near top, irregular bedding, laminated to 15 cm, calcareous cement, sharp contact with unit 1	(3.45)	4.85
1	Conglomerate, gray (N7), micrite and fine grained quartz arenite clasts, .25 to 15 cm, matrix-micrite and fine quarts sand, basal contact erosional	(1.40)	1.40

Base of Section 4

Top of Section 5

12	Quartz arenite, red (5R 5/4), very fine grained, irregular bedding, .25 to 7.5 cm, calcareous cement, sharp contact with unit 11	(.53)	29.54
11	Quartz arenite, red (10R 6/6), very fine grain to silt, thin bedded to 1 cm, calcareous cement	(1.22)	29.01

Unit no.	Description	Unit Thickness (meters)	Cumulative Thickness (meters)
10	Covered interval	(2.74)	27.79
9	Quartz arenite, reddish brown (10R 5/4), very fine grained, bedding 7.5 to 10 cm, siliceous cement . . .	(.30)	25.05
8	Covered interval	(6.10)	24.75
7	Claystone, gray (N7), contains carbonaceous horizon, up to 7.5 cm thick, near top which was sampled for geochem, irregular bedding (bioturbated ?), calcareous cement .	(1.14)	18.65
6	Covered interval	(4.32)	17.51
5	Claystone, gray (N5), irregular bedding (bioturbated ?), calcareous cement, sharp contact with unit 4 .	(3.28)	13.19
4	Carbonaceous seam, bands of carbonaceous material interbedded with beds of detrital silt and clay, numerous bands of limonite, occasional bands of azurite and malachite, selenite gypsum very common, grades into unit 3.	(1.19)	9.91
3	Siltstone, gray (N7) and reddish-brown (10R 5/4), interbedded, laminated to thin-bedded, calcareous cement	(3.89)	8.72
2	Covered interval	(3.20)	4.83
1	Conglomerate, gray (N6), micrite and fine grained quartz arenite clasts, .25 to 7.5 cm, matrix-micrite and fine quartz sand, lenticular interbeds up to 10 cm thick, same composition as matrix, basal contact erosional . .	(1.63)	1.63

Base of Section 5

Promontory Butte

Access: State 260 east of Payson; Promontory Butte 15' quadrangle; turn to north in east 1/2 sec. 26, T. 11 N., R. 12 E., opposite Boy Scout Ranch. Section 1 at cut near center of sec. 24. Section 2 at smaller cut 1/2 mile to the west.

Top Section 1

Unit no.	Description	Unit Thickness (meters)	Cumulative Thickness (meters)
7	Quartz arenite, purple (5RP 6/2) to red (10R 5/4), fine to very fine grained, very lensy, with lenses up to 60 cm, basal contact erosional, unit appears to be stream channel cut into unit 6	(3.05)	25.93
6	Quartz arenite, gray (N6) and purple (5RP 6/2), interbedded, fine to very fine grained, thin-bedded, calcareous cement sharp contact with unit 5	(5.50)	22.88
5	Quartz arenite, red (5R 4/6), fine to very fine grained, irregular bedding, .5 to 2.5 cm, calcareous cement, gradational to unit 4	(1.22)	17.38
4	Claystone, gray (N6), limonite staining common, red interbeds (unit 5) near upper contact, carbonaceous bed 5 to 15 cm thick with minor malachite, irregular bedding .25 to 7.5 cm, calcareous cement, gradational to unit 3.	(3.05)	16.16

Unit no.	Description	Unit Thickness (meters)	Cumulative Thickness (meters)
3	Light gray (N7) to dark gray (N5), unit fines upward and lithologies within it are very lensy; lowest lithology-conglomerate, micrite, claystone and quartz arenite clasts, matrix-micrite, bedding massive, next lithology--fine to very coarse sand, composition of sand same as clasts, calcareous cement; next lithology--arenaceous claystone, fine to very fine quartz sand, minor carbonaceous material and minor pyrite, locally carbonaceous material up to 10 cm thick and contains minor halite and minor malachite, thin-bedded, calcareous cement, erosional contact with unit 2	(6.10)	13.11
2	Quartz arenite, gray (N6) to purple (5RP 6/2), fine to very fine grained, minor clay, bedding .25 to 7.5 cm, calcareous cement, gradational (?) to unit 1	(3.66)	7.01
1	Conglomerate, gray (N7), weathers (10YR 6/6), micrite, claystone and quartz arenite clasts, .25 to 5 cm, matrix-micrite and fine quartz sand, unit contains lenses of arenite, fine grained, same color and lithology as conglomerate, abundant evidence of organic (plant) remains and minor sulfides, abundant iron oxide staining, individual lenses 10 to 100 cm thick, ripple marks present on upper surface of unit, basal contact erosional . .	(3.35)	3.35

Base of Section 1

Top Section 2

Unit no.	Description	Unit Thickness (meters)	Cumulative Thickness (meters)
3	Conglomerate, gray (N5), micrite and claystone clasts, .25 to 3.5 cm, matrix-micrite, contains minor malachite and pyrite, quartz arenite lenses up to 10 cm, basal contact erosional	(1.42)	5.03
2	Siltstone, gray (N6), contains carbonaceous material, azurite and malachite, especially on bedding planes, contains quartz arenite lenses, light gray (N7), fine grained, calcareous cement, up to 50 cm thick, unit is thin bedded, calcareous cement, sharp contact with unit 1	(2.90)	3.61
1	Conglomerate, gray (N5), micrite and claystone clasts, .25 to 5 cm, matrix-micrite, basal contact erosional . .	(.71)	.71

Turkey Mountain

Access: State 260 east of Payson; Woods Canyon 15' quadrangle; junction to SE in sec. 34, T. 11 N., R. 13 E. is Colcord Road; small prospect pit to north about 100 yds. and just west of local access road to north in SE 1/4, SE 1/4 sec. 35.

Unit no.	Description	Unit Thickness (meters)	Cumulative Thickness (meters)
4	Conglomerate, purple (5RP 6/2) weathers gray (N7), micrite pebbles, matrix-micrite and fine grained quartz sand, contains fine grained quartz sand lenses up to 15 cm, becomes more sandy and less conglomeratic near top	(1.55)	4.68
3	Covered interval.	(.97)	3.13

Unit no.	Description	Unit Thickness (meters)	Cumulative Thickness (meters)
2	Quartz arenite, light gray (N7), fine grained, contains azurite, malachite, hematite and carbonaceous material on bedding planes, thin-bedded, calcareous cement, sharp contact with unit 1	(1.70)	2.16
1	Conglomerate, gray (N4), micrite and claystone clasts, .25 to 10 cm, matrix-micrite and fine grained quartz sand, contains fine grained quartz sand lenses up to 10 cm thick, limonite, azurite, malachite, hematite and plant remains present	(.46)	.46

APPENDIX B

INITIAL SOLUTION COMPOSITIONS
(log total molality of elements)

	Al	K	Na	Ca	S	Cu
Brine	-9.0000	- .8928	.4771	- .1871	-2.2218	- 6.0000
Groundwater	-9.4306	-3.2306	-3.5171	-2.8447	-3.5229	-14.0000

	S:	Fe	C	Cl	O	H
Brine	-4.1871	-5.0000	-4.0000	.6450	1.7446	2.0454
Groundwater	-4.0132	-9.0872	-2.5229	-3.4858	1.7444	2.0454

	pH	Temperature	Log fO_2
Brine	5.500	25°C	-64.587
Groundwater	7.500	25°C	-64.560

REFERENCES

Bastin, E. S., 1950, Interpretation of ore textures: Geol. Soc. America Mem. 45, 101 p.

Bathurst, R. G. C., 1966, Boring algae, micrite envelopes and lithification of molluscan biosparites: Geol. Jour., v. 5, pt. 1, pp. 15-32.

Blazey, E. B., 1971, Fossil flora of the Mogollon Rim: Ph. D. Dissertation, Arizona State University, 169 p.

Bressler, S. L., 1977, Research Assist., The Univ. of Ariz., Pers. Com.

Brew, D. C., 1965, Stratigraphy of the Naco Formation (Pennsylvanian) in central Arizona: Ph. D. Dissertation, Cornell University, 201 p.

Carpenter, A. B., Trout, M. L. and Pickett, E. E., 1974, Preliminary report on the origin and chemical evolution of lead- and zinc-rich oil field brines in central Mississippi: Econ. Geol., v. 69, pp. 1191-1206.

Conyers, L. B., 1975, Depositional environments of the Supai Formation in central Arizona: M. S. Thesis, Arizona State University, 124 p.

Davies, G. R., 1970, Algal-laminated sediments, Gladstone embayment, Shark Bay, Western Australia: Am. Assoc. Petroleum Geologists, Mem. 13, pp. 169-205.

Entwistle, L. P. and Louin, L. O., 1955, The chalcocite-ore deposits at Corocoro, Bolivia: Econ, Geol., v. 50, pp. 555-570.

Garrels, R. M. and Christ, C. L., 1965, Solutions, Minerals and Equilibria: Freeman, Cooper and Co., San Francisco, California, 450 p.

Harms, J. C., Southard, J. B., Spearing, D. R., and Walker, R. T., 1975, Depositional environments as interpreted from primary sedimentary structures and stratification sequence: Soc. Econ. Paleontologists and Mineralogists Short Course 2, 161 p.

Helgeson, H. C., Brown, T. H., Nigrini, A., and Jones, T. A., 1970, Calculation of mass transfer in geochemical processes involving aqueous solutions: Geochim. et Cosmochim. ACTA, v. 34, pp. 569-592.

Huddle, J. W. and Dobrovolny, E., 1945, Late Paleozoic stratigraphy and oil and gas possibilities of central and northeastern Arizona: U. S. Geol. Survey Oil and Gas Invest. Prelim. Chart 10.

_____, 1952, Devonian and Mississippian rocks of Central Arizona: U. S. Geol. Survey Prof. Paper 233-D, pp. 67-112.

Jackson, R. L., 1951, The stratigraphy of the Supai Formation along the Mogollon Rim, central Arizona: M. S. Thesis, The University of Arizona, 82 p.

Jones, N. O., 1977, Uranium, copper and vanadium content of selected arenaceous sediments from the lower Supai Formation, Mogollon Rim, Arizona: M. S. Thesis, The University of Arizona, 126 p.

Knight, J. E., 1976, A thermodynamic study of alunite and copper-arsenic sulfosalt deposits: M. S. Thesis, The University of Arizona, 142 p.

Lokke, D. H., 1962, Palentological reconnaissance of subsurface Pennsylvanian in southern Apache and Navajo Counties, Arizona: N. Mex. Geol. Soc. 13th Field Conf. Guidebook, pp. 84-86.

Love, L. G., 1969, Sulfides of metals in recent sediments: In James, C. H., Ed., Sedimentary Ores ancient and modern: Sp. Pub. No. 1, Dept. of Geol., Univ. of Leicester, pp. 31-60.

McGoon, D. O., 1962, Occurrences of Paleozoic carbonaceous deposits in the Mogollon Rim region: N. Mex. Geol. Soc., Guidebook 13th Field Conf., pp. 89-91.

McKee, E. D., 1938, Environment and history of the Toroweap and Kaibab Formations of northern Arizona and southern Utah: Carnegie Inst. Washington Pub. 492, 268 p.

McKee, E. D. and Gutschick, R. C., 1969, History of the Redwall Limestone of southeastern Arizona: Geol. Soc. America Mem. 114, 693 p.

Peirce, H. W., Jones, N. and Rogers, R., 1977, A survey of uranium favorability of Paleozoic Rocks in the Mogollon Rim and Slope region--East Central Arizona: State of Ariz., Bur. of Geol. and Mineral Tech., Univ. of Ariz., Circular 19, 71 p.

Ransome, F. L., 1916, Some Paleozoic Sections in Arizona and their correlation: U. S. Geol. Survey Prof. Paper 98, pp. 133-166.

Reinack, H. E. and Wunderlich, F., 1968, Classification and origin of flaser and lenticular bedding: Sedimentology, v. 11, pp. 99-104.

Ross, C. A., 1973, Pennsylvanian and Early Permian depositional history, Southeastern Arizona: Am. Assoc. Petroleum Geologists Bull., v. 57, pp. 887-912.

Sabels, B. E., 1962, Mogollon Rim volcanism and geochronology: N. Mex. Geol. Soc., 13th Field Cont., pp. 100-106.

Scherer, M., 1976, Influences of diagenetic environment on porosity and permeability of Holocene and pleistocene corals: Am. Assoc. Petroleum Geologists Bull., v. 60, pp. 2153-2159.

Shafiqullah, M., 1977, Research Assoc., The Univ. of Ariz., Pers. Com.

Shride, A. F., 1967, Younger Precambrian geology in Southeastern Arizona: U. S. Geol. Survey Prof. Paper 566, 89 p.

Swanson, V. E., Love, A. H., and Frost, I. C., 1972, Geochemistry and diagenesis of tidal-marsh sediments, northeastern Gulf of Mexico: U. S. Geol. Survey Bull. 1360, 83 p.

Teichert, C., 1965, Devonian rocks and paleogeography of central Arizona: U. S. Geol. Survey Prof. Paper 464, 181 p.

Titley, S. R., 1962, Geology along the Diamond Rim and adjoining areas, Gila and Navajo Counties, Arizona: N. Mex. Geol. Soc. 13th Field Conf. Guidebook, pp. 123-128.

Winters, S. S., 1963, Supai Formation (Permian) of eastern Arizona: Geol. Soc. America Mem. 89, 99 p.